

A STUDY OF DYNAMIC CRACK INSTABILITIES USING COHESIVE CONTINUUM METHODS

P.A. Klein and T.D. Nguyen

Sandia National Laboratories, Livermore, CA 94550, USA

ABSTRACT

Though classical approaches to fracture, based on small deformation theory, have been applied successfully to a wide range of applications, they may be inapplicable for explaining experimental observations in which nonlinear, hyperelastic material response is an essential feature of the phenomenon. Among these phenomena are the branching instabilities observed during dynamic crack propagation. Simulation approaches that incorporate a cohesive view of material are able to demonstrate the appearance of fracture path instabilities. In this work, we study the hypothesis that instabilities occur as a result of a local limiting speed by investigating dynamic crack propagation along a weak plane in a strip described by a cohesive continuum. The introduction of the weak plane allows the fracture properties and the properties of the strain-softened, near-tip region to be selected independently. In the absence of dissipation, a mode I crack in a strip should accelerate to the Rayleigh wave speed if the far-field driving force exceeds the fracture energy. Under these conditions, the local limiting speed hypothesis predicts that the crack speed will be dictated not by the far-field driving force, but by acoustic wave speeds in the region surrounding the crack tip. It then follows that a crack that is unable to accelerate will become surrounded by a growing region of accumulating strain energy. The goal of this work is to study what effect the strain energy accumulating in the near-tip region has on the onset of branching instabilities. The scale and structure of this region will be investigated by evaluating the energy-momentum flux through various contours around the moving crack tip.

1 INTRODUCTION

Most existing theories of brittle fracture are based on a small deformation description of material behavior. These approaches neglect the extraordinarily large, nonlinear elastic deformations that inevitably occur near the crack tip, and assume that the crack initiation and propagation characteristics can be determined solely from the mechanical state of the far-field. However, recent experimental observations of dynamic crack propagation in nominally brittle materials (see [1]) have challenged this global viewpoint. Small deformation theories have been unable to predict such fundamental results as the relationship between the crack speed and driving force, the maximum crack speed, and development of branching instabilities. Experiments consistently report the maximum crack speed at roughly half of the theoretical limiting value, the Rayleigh wave speed (c_R), and fracture path instabilities have been observed at speeds as low as $c_R/3$ [2]. Ravi-Chandar and Knauss [3] performed a series of experiments to observe dynamic crack propagation in Homalite, a brittle polymer. Though the experiments were designed to drive the crack to the theoretical limiting speed, they observed terminal crack speeds between $0.35c_R - 0.5c_R$ depending on the loading rate. From analyses of the fracture surface, they also observed progressive roughening with crack extension preceding branching. These results led Ravi-Chandar and Knauss to conclude that the excess driving force, beyond what is needed to propagate the crack at the driving force is absorbed by large deformation material processes in the near tip region, specifically the nucleation and growth of microcracks, that lead to the development of fracture path instabilities.

Though explanations for the development of dynamic instabilities have been sought within the classical, small deformation, elastodynamic framework (see for example [4]), none can predict the

onset of fracture path instabilities at the low speeds observed in experiments [1]. This led Gao [5, 6] to propose that a local viewpoint, one that considers the nonlinear, hyperelastic material response in the near-tip region, is essential for understanding the dynamics of crack propagation and the development of fracture path instabilities. Using a hyperelastic, strain-softening model to describe the material response ahead of a Mode I crack tip, Gao showed that the elastic wave speeds at the cohesive state are severely reduced by hyperelastic softening from those exhibited in the nearly undeformed, far-field material. The severe deformation in the near-tip region creates a zone of highly stressed, strain-softened material that slows the flow of energy to material ahead of the crack tip. The speed of crack propagation is ultimately limited by the rate of energy transport through the slow zone, characterized by the locally reduced wave speeds, and not the globally applied driving force. The local limiting speed hypothesis provides an explanation for the occurrence of dynamic instabilities. With the wave speeds severely reduced ahead of the crack tip, the crack seeks alternate propagation directions along which the material exhibits less softening and energy can be delivered at a faster rate. The result is a wavy propagation path that corresponds to the roughened appearance of the fracture surface. For a crack traveling near the local limiting speed, the rate of energy transport to the crack tip to sustain the fracture process can lag the energy flux into the nonlinear zone. The accumulation of energy that would have otherwise gone to accelerating crack growth causes the material inside the slow zone to become more highly stressed and the slow zone itself to enlarge.

The Virtual Internal Bond (VIB) model was developed by Gao and Klein [7] to introduce the effects of hyperelastic softening at the crack tip. VIB is fundamentally an extension of Cauchy-Born elasticity to an isotropic network of material particles joined by phenomenological bonds. The bonds deform according to the macroscopic deformation gradient, and the interactions of the bonds are averaged over the network distribution to calculate the continuum strain energy density for manipulation by hyperelasticity theory. The constitutive relations of VIB exhibit strain softening if a cohesive force law is used to describe the behavior of the bonds. Though VIB conceptually represents the “damage” sustained (for example, by microcracking) in the near-tip region, it is different from a continuum damage model which produces strain softening through the evolution of an internal history variable representing the state of material damage. Instead, the material softens continuously with deformation as dictated by the cohesive potential. VIB has been applied successfully to simulate the development of dynamic instabilities. For example, Klein and Gao [8] use VIB to simulate the dynamic fracture experiments of Fineberg and coworkers [9]. A prediction of the branching pattern under dynamic crack growth conditions is shown in Figure 1. The simulation models crack

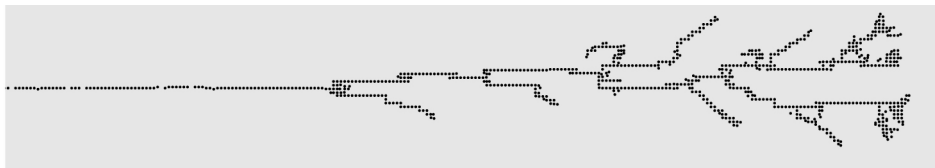


Figure 1: A pattern of dynamic crack branching predicted using the Virtual Internal Bond model [8].

propagation in a long strip subject to constant rate displacement of the upper and lower edges. For a range of applied boundary velocities, the crack quickly accelerates to a terminal speed that does not exceed $0.53c_R$, and instabilities in the crack speed appear at $0.32c_R$. Also, a slow zone appears at the crack tip and grows as the crack accelerates to the terminal speed and during extension at the terminal speed. Prolonged propagation at the terminal speed results in branching.

The development of the near tip nonlinear zone and the role it plays in triggering crack tip instabilities and branching have not been investigated in detail. It is traditionally considered that a necessary condition for crack branching is that the energy release rate be sufficient for providing the dissipation associated with the creation of four free surfaces, two for each fracture path. This condition is derived from a global viewpoint of the energy balance. With the introduction of a cohesive continuum, a crack that macroscopically appears to be propagating under steady-state conditions may be developing a local accumulation of strain energy around the crack tip. This accumulated strain energy may then drive the development of branching at a small scale that is not admissible from the global viewpoint. In order to study these effects, we consider the case of a crack propagating under constant far-field loading conditions along a weak plane in a strip of material whose properties are given by a cohesive continuum model. For this configuration, Liu and Marder [10] showed that the crack will accelerate to the Rayleigh wave speed for any applied driving force exceeding the fracture energy, exhibiting a characteristic transient time governed by the loading, strip geometry, and material properties. A weak plane is introduced so the properties of the strain-softened near tip region can be selected independently of the fracture properties. We will study the scale and structure of the zone accumulating strain energy using the material force method, following the framework introduced by Maugin and Trimarco [11]. The method can be used to calculate the flux of energy-momentum across different contours around the crack tip. As a result, we will be able to assess the size of the zone of strain energy accumulation and determine how this zone contributes to the development of crack tip instabilities. The components of our modeling approach are described briefly below.

2 THE VIRTUAL INTERNAL BOND MODEL

The VIB model is developed within the framework of hyperelasticity. The arrangement of cohesive interactions among material particles is described by a bond density function. The strain energy density,

$$\Phi = \frac{1}{\Omega_0} \int_{\Omega_0^*} U(r) D_\Omega d\Omega, \quad (1)$$

is computed by integrating the bond density over a representative volume in a continuous analog to the sum over discrete lattice neighbors for the case of crystalline materials. The variables Ω_0 is the undeformed representative volume, r is the deformed virtual bond length, $U(r)$ is the bonding potential, D_Ω is the volumetric bond density function, and Ω_0^* is the integration volume defined by the range of influence of U . This method was first alluded to by Gao [5] for constructing an amorphous network of cohesive bonds by a spatial average. The deformed bond length r is computed from the Cauchy-Born rule, assuming affine deformation of the integration volume Ω_0^* . In order to avoid questions as to whether the Cauchy-Born rule holds for the proposed microstructure, we consider only bond density functions D_Ω that are centrosymmetric. Under this restriction, the deformation at the microstructural level must be homogeneous in order to maintain the symmetry present in the undeformed configuration. The undeformed virtual bond vector is represented as, $\mathbf{R} = R \mathbf{E}$, where R is the reference bond length, and \mathbf{E} is a unit vector in the direction of the undeformed bond. Undeformed bonds are mapped to their deformed configuration \mathbf{r} by the affine transformation, $\mathbf{r} = \mathbf{F} \mathbf{R}$ where \mathbf{F} is the continuum deformation gradient. Making use of the right Cauchy-Green stretch tensor, the deformed bond length is calculated as

$$r(\mathbf{C}) = R \sqrt{\mathbf{E} \cdot \mathbf{C} \mathbf{E}}. \quad (2)$$

Using hyperelasticity theory, the stress response is computed from the strain energy density (1) as,

$$\mathbf{S} = 2 \frac{\partial \Phi}{\partial \mathbf{C}} = \frac{1}{\Omega_0} \int_{\Omega_0^*} \frac{U'(r)}{r} \mathbf{E} \otimes \mathbf{E} R^2 D_\Omega d\Omega, \quad (3)$$

where \mathbf{S} is the the (symmetric) 2nd Piola-Kirchhoff stress tensor. Selecting the centrosymmetric bond distribution function as $D_\Omega = D_0 \delta_D(R - R_0)$, where D_0 is a constant and δ_D is the Dirac delta function, yields a model for amorphous material with nearest neighbor bonding only.

3 THE COHESIVE SURFACE METHOD

The weak plane in our system is modeled using a cohesive surface approach. The advantage of this approach is that crack advance occurs, without requiring evaluation of a fracture criterion, as dictated by the local driving force. For this study, we use a traction-separation relation similar to the one introduced by Tvergaard and Hutchinson [12]. The magnitude of the cohesive traction is expressed as a function of a nondimensional effective opening displacement

$$\Delta = \sqrt{(\Delta_t/\delta_t^*)^2 + (\Delta_n/\delta_n^*)^2}, \quad (4)$$

where δ_t^* and δ_n^* represent the characteristic tangential and normal opening displacements, respectively. Defining the traction potential

$$\varphi(\mathbf{\Delta}) = \delta_n^* \int_0^\Delta \hat{T}(\xi) d\xi \quad (5)$$

yields the rate-independent, mixed-mode traction-separation relation

$$\mathbf{T}(\mathbf{\Delta}) = \frac{\partial \varphi(\mathbf{\Delta})}{\partial \mathbf{\Delta}} = \delta_n^* \hat{T}(\Delta) \frac{\partial \Delta}{\partial \mathbf{\Delta}}. \quad (6)$$

For simplicity, we select a simple tri-linear form for $\hat{T}(\Delta)$, characterized by a cohesive stress $\sigma_c = \hat{T}(\Delta^*)$ where $0 < \Delta^* < 1$, yielding a fracture energy $G_c = \frac{1}{2} \sigma_c \delta_n^*$. The cohesive stress will be selected to drive deformation of the surrounding material well into the nonlinear regime, while the length parameter δ_n^* will be selected to ensure the scale of the nonlinear near-tip zone is well-resolved by the mesh.

4 DISCUSSION

Figure 2 shows the development of the initial branch in a crack propagating through a strip of material described by the VIB model, as presented in [8]. Locations at which the acoustic wave speeds have dropped below a critical value are indicated with dark points. The strip is loaded by a constant boundary velocity, and the times shown are normalized by the time at which the crack begins to propagate. Initially (a), all points displaying localization lie along a straight path extending from the pre-crack. After $t/t_{\text{init}} = 1.28$ (b), the first evidence of localization above and below the symmetry line appears. Based on the local limiting speed theory of dynamic crack tip instabilities, the crack has reached a speed at which the strain-softened material immediately ahead of the crack is unable to

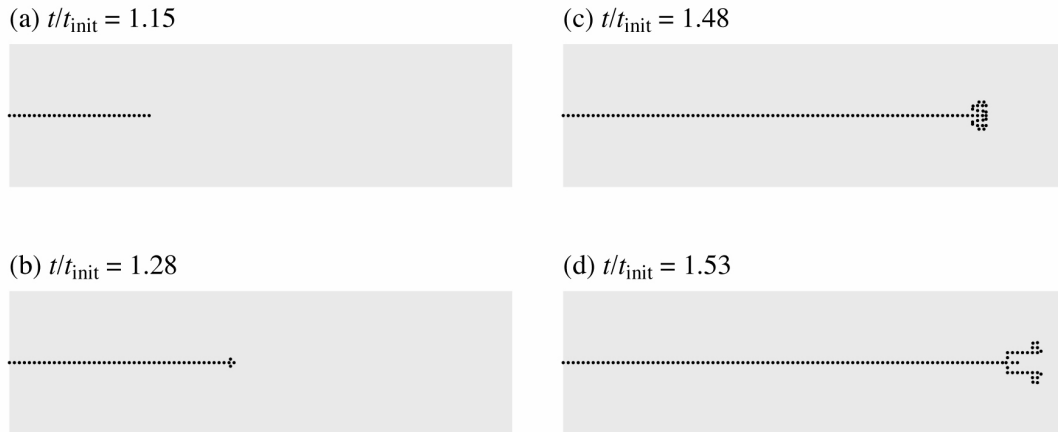


Figure 2: The onset of branching instability.

maintain a sufficient rate of energy transfer, and the crack has begun to probe alternate propagation directions. Between $1.28 < t/t_{\text{init}} < 1.48$ (c), the crack continues to accelerate and the acoustical barrier ahead of the crack tip enlarges, evolving to an extended region of “slow” material. Since deformations in the VIB model are strictly reversible, the material recovers as the tip moves away, leaving no indication of this extended region in the subsequent fracture path. At some time before $t/t_{\text{init}} = 1.53$ (d), the crack tip reaches a critical state, and the first true branch appears in the crack path.

This calculation illustrates the development of a branching instability, but characteristics of the near tip zone were not investigated. In part, this omission is due to the limitation imposed by the absence of a weak plane. Without a weak plane, the fracture properties and the nonlinear elastic behavior of the continuum are intimately linked by the characteristics of the VIB model, which limited mesh resolution of the near-tip zone. The loading in this calculation was also applied too quickly to allow the near tip zone to develop under a nearly constant far-field driving force. Indeed, since the far-field driving force scales with the square of the applied nominal strain and thus as $(t/t_{\text{init}})^2$, the branching seen in Figure 2 occurs after the far-field driving force exceeds twice the fracture energy. We will address these limitations in the previous study to clarify the effect of the near tip nonlinear zone.

ACKNOWLEDGMENTS

Sandia is a multiprogram laboratory operated by Sandia Corporation, a Lockheed Martin Company, for the United States Department of Energy’s National Nuclear Security Administration under contract DE-AC04-94AL85000.

References

- [1] Ravi-Chandar, K., Dynamic fracture of nominally brittle materials, *International Journal of Fracture* 90 (1998) 83–102.

- [2] Fineberg, J., Gross, S. P., Marder, M., Swinney, H. L., Instability in the propagation of fast cracks, *Physical Review B* 45 (1992) 5146–5154.
- [3] Ravi-Chandar, K., Knauss, W. G., An experimental investigation into dynamic fracture: III. On steady-state crack propagation and crack branching, *International Journal of Fracture* 26 (1984) 141–154.
- [4] Yoffe, E. H., The moving Griffith crack, *Philosophical Magazine* 42 (1951) 739–750.
- [5] Gao, H. J., A theory of local limiting speed in dynamic fracture, *Journal of the Mechanics and Physics of Solids* 44 (1996) 1453–1474.
- [6] Gao, H. J., Elastic waves in a hyperelastic solid near its plane strain equibiaxial cohesive limit, *Philosophical Magazine Letters* 76 (1997) 307–314.
- [7] Gao, H. J., Klein, P., Numerical simulation of crack growth in an isotropic solid with randomized internal cohesive bonds, *Journal of the Mechanics and Physics of Solids* 46 (1998) 187–284.
- [8] Klein, P. A., Gao, H., Study of crack dynamics using the virtual internal bond method, in: Chuang, T. J., Rudnicki, J. W. (Eds.), *Multiscale Deformation and Fracture in Materials and Structures: The James R. Rice 60th Anniversary Volume*, Kluwer Academic Publishers, Dordrecht, The Netherlands, 2000, pp. 275–309.
- [9] Fineberg, J., Gross, S. P., Marder, M., Swinney, H. L., Instability in dynamic fracture, *Physical Review Letters* 67 (1991) 457–460.
- [10] Liu, X., Marder, M., The energy of a steady-state crack in a strip, *Journal of the Mechanics and Physics of Solids* 39 (1991) 947–961.
- [11] Maugin, G. A., Trimarco, C., Pseudomomentum and material forces in nonlinear elasticity: variational formulations and application to brittle fracture, *Acta Mechanica* 94 (1992) 1–28.
- [12] Tvergaard, V., Hutchinson, J. W., The relation between crack growth resistance and fracture process parameters in elastic-plastic solids, *Journal of the Mechanics and Physics of Solids* 40 (1992) 1377–1397.